Supporting Information

Slow magnetic relaxation in a trigonal-planar mononuclear Fe(II) complex

Yuzhu Li,[a‡] Jing Xi,[a‡] Jesús Ferrando-Soria,[b] Yi-Quan Zhang,[c*] Wenyuan Wang,[d] You Song,[e] Yan Guo,[a*] Emilio Pardo [b] and Xiangyu Liu[a,e*]

[a] State Key Laboratory of High-efficiency Utilization of Coal and Green Chemical Engineering, College of Chemistry and Chemical Engineering, Ningxia University, Yinchuan 750021, China.

[b] Departamento de Química Inorgánica, Instituto de Ciencia Molecular (ICMOL), Universidad de Valencia, Paterna 46980, Valencia, Spain.

[c] Jiangsu Key Laboratory for NSLSCS, School of Physical Science and Technology, Nanjing Normal University, Nanjing 210023, China.

[d] College of Chemistry and Materials Science, Northwest University, Xi'an, Shaanxi 710069, China.

[e] State Key Laboratory of Coordination Chemistry, Nanjing University, Nanjing 210046, China

‡ These authors contributed equally to this work.

***Corresponding author**

Dr. Xiangyu Liu

E-mail: xiangyuliu432@126.com

***Corresponding author**

Dr. Yan Guo

E-mail: 452785231@qq.com

***Corresponding author**

Prof. Yi-Quan Zhang

E-mail: zhangyiquan@njnu.edu.cn

Contents:

ions of complexes **1** in their ground spin-orbit states.

Table S1. Selected crystallographic data and structure refinement for complexes **1-2**.

Complex	**1**	**2**
Empirical formula	$C_{45}H_{49}N_2Cl_2Fe$	$C_{45}H_{49}ClFeN_2$
Formula weight	744.61	709.16
Temperature	153.15	153.15
Crystal system	triclinic	orthorhombic
Space group	$P\bar{1}$	*Pnma*
a (Å)	12.604(2)	12.3687(7)
b (Å)	16.344(3)	22.9892(10)
c (Å)	20.239(4)	13.9721(6)
α (°)	94.765(7)	90
β (°)	92.058(6)	90
γ (°)	109.136(6)	90
V (Å^3)	3916.2(12)	3972.9(3)
Z	4	4
D (g/cm^3)	1.263	1.186
Mu (mm^{-1})	0.555	0.479
F(0 0 0)	1572.0	1504.0
Completeness	99.4	99.9
Unique reflections	16093	4187
Observed reflections	47592	75142
R_{int}	0.0421	0.1450
Final *R* indices[$I>2\sigma(I)$]	$R_1 = 0.0378$ $wR_2 = 0.0863$	$R_1 = 0.0598$ $wR_2 = 0.1777$
R indices (all data)	$R_1 = 0.0567$ $wR_2 = 0.0933$	$R_1 = 0.0854$ $wR_2 = 0.1932$
Goodness-of-fit on F^2	1.016	1.044

Table S2. Selected Bond Lengths (Å) and Bond Angles (°) for **1**

1			
C(1)-N(2)	1.323(2)	C(1)-N(2)-Fe(1)	117.84(12)
C(3)-N(1)	1.351(2)	C(22)-N(2)-Fe(1)	120.46(12)
C(22)-N(2)	1.460(2)	N(4)-C(46)-C(47)	123.59(16)
C(34)-N(1)	1.457(2)	N(4)-C(46)-C(61)	118.52(16)
Cl(1)-Fe(1)	2.1970(7)	N(3)-C(48)-C(47)	123.64(17)
Cl(2)-Fe(1)	2.1825(7)	N(3)-C(48)-C(49)	118.90(16)
Fe(1)-N(1)	1.9432(17)	C(68)-C(67)-N(4)	119.92(17)
Fe(1)-N(2)	1.9837(16)	Cl(4)-Fe(2)-Cl(3)	115.31(3)
C(46)-N(4)	1.333(2)	N(3)-Fe(2)-Cl(3)	104.77(5)
C(48)-N(3)	1.350(2)	N(3)-Fe(2)-Cl(4)	117.96(5)
C(67)-N(4)	1.463(2)	N(3)-Fe(2)-N(4)	94.63(7)
C(79)-N(3)	1.457(2)	N(4)-Fe(2)-Cl(3)	108.50(5)
Cl(3)-Fe(2)	2.2052(7)	N(4)-Fe(2)-Cl(4)	113.43(5)
Cl(4)-Fe(2)	2.1810(7)	C(48)-N(3)-C(79)	119.74(15)
Fe(2)-N(3)	1.9511(16)	C(48)-N(3)-Fe(2)	113.(79)(13)
Fe(2)-N(4)	1.9832(16)	C(79)-N(3)-Fe(2)	125.64(12)
N(2)-C(1)-C(2)	123.78(17)	C(46)-N(4)-C(67)	119.53(15)
N(2)-C(1)-C(16)	120.66(17)	C(46)-N(4)-Fe(2)	115.76(12)
N(1)-C(3)-C(2)	122.98(17)	C(67)-N(4)-Fe(2)	122.89(11)
N(1)-C(3)-C(4)	119.59(16)	C(2)-C(1)-N(2)-Fe(1)	3.8(2)
C(23)-C(22)-N(2)	118.55(17)	C(2)-C(3)-N(1)-Fe(1)	32.9(2)
C(27)-C(22)-N(2)	120.18(18)	C(4)-C(3)-N(1)-Fe(1)	146.76(14)
C(35)-C(34)-N(1)	117.22(18)	C(16)-C(1)-N(2)-Fe(1)	178.58(13)
C(39)-C(34)-N(1)	120.61(18)	C(23)-C(22)-N(2)-Fe(1)	77.4(2)
Cl(2)-Fe(1)-Cl(1)	116.10(3)	C(27)-C(22)-N(2)-Fe(1)	99.18(19)
N(1)-Fe(1)-Cl(1)	107.32(5)	C(35)-C(34)-N(1)-Fe(1)	96.83(19)
N(1)-Fe(1)-Cl(2)	114.28(5)	C(39)-C(34)-N(1)-Fe(1)	83.5(2)
N(1)-Fe(1)-N(2)	94.63(7)	C(47)-C(46)-N(4)-Fe(2)	16.0(2)
N(2)-Fe(1)-Cl(1)	109.16(5)	C(49)-C(48)-N(3)-Fe(2)	148.75(14)
N(2)-Fe(1)-Cl(2)	113.18(5)	C(61)-C(46)-N(4)-Fe(2)	166.24(13)
C(3)-N(1)-C(34)	119.11(16)	C(68)-C(67)-N(4)-Fe(2)	97.06(19)
C(3)-N(1)-Fe(1)	114.86(13)	C(72)-C(67)-N(4)-Fe(2)	81.62(19)
C(34)-N(1)-Fe(1)	123.44(12)	C(80)-C(79)-N(3)-Fe(2)	112.05(18)
C(1)-N(2)-C(22)	121.69(16)	C(84)-C(79)-N(3)-Fe(2)	65.2(2)

Table S3. Selected Bond Lengths (Å) and Bond Angles (°) for **2**

2			
Fe(1)-Cl(1)	2.1860(15)	C1[1]-C(2)-C(1)	125.7(3)
Fe(1)-N(1)	1.960(2)	C1-C(2)-C(25)	117.13(17)
Fe(1)-N(1)[1]	1.960(2)	C(1)[1]-C(2)-C(25)	117.13(13)
N(1)-C(1)	1.329(3)	Fe(1)-N(1)-C(1)-C2	-3.9(4)
N(1)-C(10)	1.449(3)	Fe(1)-N(1)-C(1)-C(19)	178.0(6)
C(1)-C(2)	1.413(3)	Fe(1)-N(1)-C(10)-C(11)	-86.1(3)
C(1)-C(19)	1.473(9)	Fe(1)-N(1)-C(10)-C(15)	89.9(3)
C(1)-C(19A)	1.547(10)	N(1)-C(1)-C2-C(1)[1]	-0.5(6)
C(2)-C(25)	1.513(5)	N(1)-C(1)-C2-C25	-179.8(3)
N(1)-Fe(1)-Cl(1)	133.60(7)	N(1)-C(1)-C(19)-C20	-103.3(8)
N(1)A[1]-Fe(1)-Cl(1)	133.60(7)	N(1)-C(1)-C(19)-C24	80.3(8)
N(1)A[1]-Fe(1)-N(1)	92.80(13)	N(1)-C(1)-C(19A)-C(24A)	89.1(9)
C(1)-N(1)-Fe(1)	126.46(18)	N(1)-C(1)-C(19A)-C(20A)	-91.9(8)
C(1)-N(1)-C(10)	120.4(2)	N(1)-C(10)-C(11)-C(8)	-0.8(4)
C(10)-N(1)-Fe(1)	113.02(17)	N(1)-C(10)-C(11)-C(12)	177.4(3)
N(1)-C(1)-C(2)	124.1(2)	N(1)-C(10)-C(15)-C(14)	-178.5(3)
N(1)-C(1)-C(19)	118.8(5)	N(1)-C(10)-C(15)-C(17)	-1.2(4)
N(1)-C(1)-C(19A)	118.5(7)	C(1)-N(1)-C(10)-C(11)	89.4(3)
[1]+X,1/2-Y,+Z			

Table S4. Relaxation fitting parameters from least-squares fitting of $\chi(f)$ data under 1500 Oe dc field of **2**.

T(K)	χ_T	χ_S	α
3	0.435	1.95×10^{-2}	0.193
3.5	0.403	2.10×10^{-2}	0.185
4	0.363	2.22×10^{-2}	0.171
4.5	0.331	2.24×10^{-2}	0.162
5	0.302	2.36×10^{-2}	0.143
5.2	0.291	2.41×10^{-2}	0.134
5.5	0.276	2.44×10^{-2}	0.122
5.8	0.263	2.42×10^{-2}	0.112
6	0.254	2.51×10^{-2}	0.100
6.2	0.247	2.41×10^{-2}	9.73×10^{-2}
6.5	0.236	2.43×10^{-2}	8.45×10^{-2}
6.8	0.226	2.30×10^{-2}	7.68×10^{-2}
7	0.220	2.32×10^{-2}	6.82×10^{-2}
7.2	0.214	2.33×10^{-2}	5.92×10^{-2}
7.5	0.206	2.15×10^{-2}	5.12×10^{-2}
7.8	0.198	1.87×10^{-2}	4.48×10^{-2}
8	0.194	1.62×10^{-2}	4.59×10^{-2}
8.5	0.183	1.48×10^{-2}	4.61×10^{-2}
9	0.174	1.44×10^{-2}	4.31×10^{-2}
9.5	0.165	1.05×10^{-2}	3.79×10^{-2}
10	0.156	8.85×10^{-3}	4.67×10^{-2}
11	0.143	7.58×10^{-3}	4.11×10^{-2}
12	0.132	6.35×10^{-3}	4.25×10^{-2}

Table S5. Contributions of the excited states (with relative energy cm^{-1}) to D value (cm^{-1}) for **2** using CASSCF/RASSI-SO with ORCA 4.2.

	State No.	Mult	Energy, cm^{-1}	Contribution, cm^{-1}
				D
2	1	5	238.9	−61.8
	2	5	2708.3	4.3

Table S6. Relative energies (cm^{-1}) of ligand field one-electron states (in the basis of d-AOs) of **1*a*, 1*b*** and **2** from AILFT analysis using CASSCF/RASSI-SO with ORCA 4.2.

	No.	LF one-electron state	Energy, cm^{-1}
	1	0.85 d_{xz}+ 0.48 d_{x2-y2} + 0.14 d_{xy}	0.0
	2	– 0.81d_{x2-y2} + 0.51d_{xz} – 0.26 d_{yz}	307.6
1*a*	3	– 0.82 d_{z2} + 0.57 d_{yz}	5381.5
	4	– 0.76 d_{yz} – 0.55 d_{z2} + 0.32d_{x2-y2}	6720.5
	5	– 0.98d_{xy} + 0.14 d_{z2}	9540.5
	1	– 0.69 d_{xy} – 0.62 d_{xz} – 0.24 d_{yz}	0.0
	2	– 0.56 d_{xz} + 0.55 d_{yz} + 0.55 d_{x2-y2}	781.9
1*b*	3	– 0.91 d_{z2} – 0.34 d_{yz} – 0.13 d_{xz}	5161.3
	4	0.76 d_{x2-y2} – 0.62 d_{yz}	6724.8
	5	– 0.69 d_{xy} + 0.51d_{xz} + 0.37 d_{yz}	9505.8
	1	– 0.99 d_{yz}	0.0
	2	0.98 d_{z2} + 0.20 d_{x2-y2}	44.5
2	3	– 0.99 d_{xz}	2398.1
	4	0.98 d_{x2-y2} – 0.20 d_{z2}	4255.2
	5	– 0.99 d_{xy}	11310.9

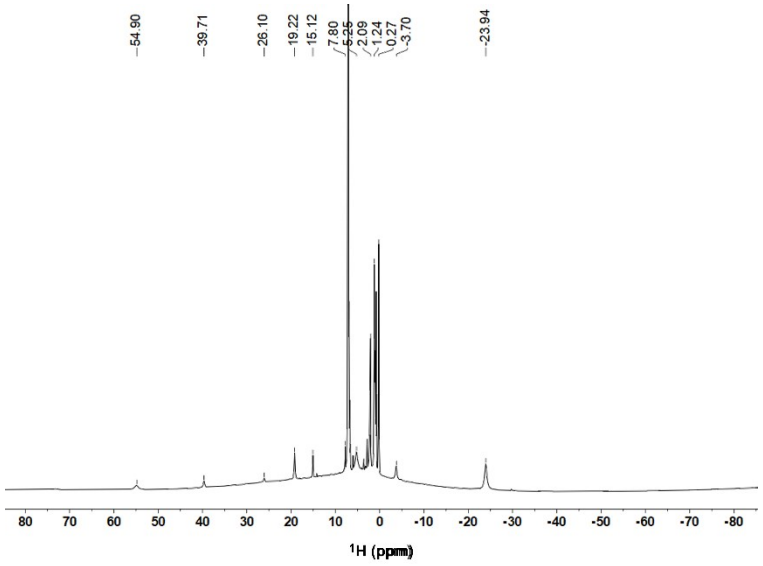

Fig. S1 ^{1}H NMR spectrum of **2** in benzene-d_6.

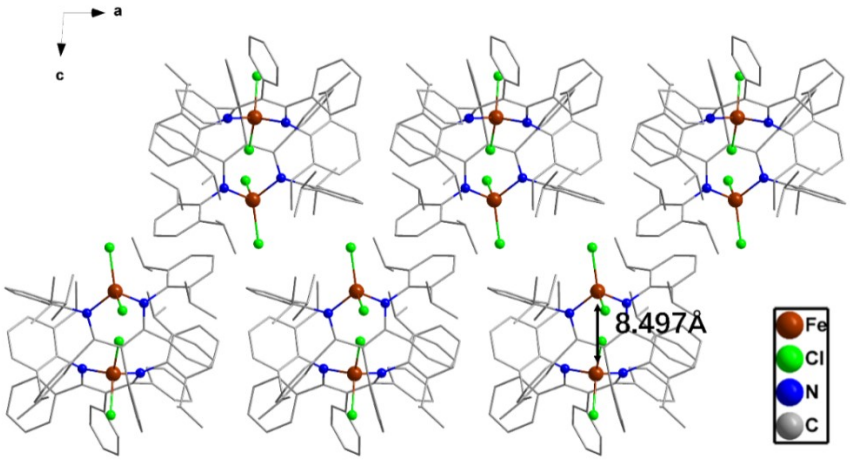

Fig. S2 Packing arrangement of **1** along the crystallographic *b* axis.

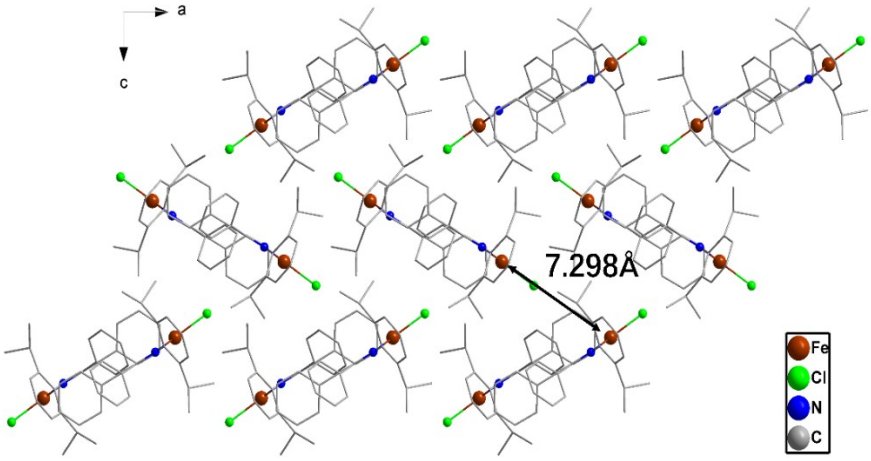

Fig. S3 Packing arrangement of **2** along the crystallographic *b* axis.

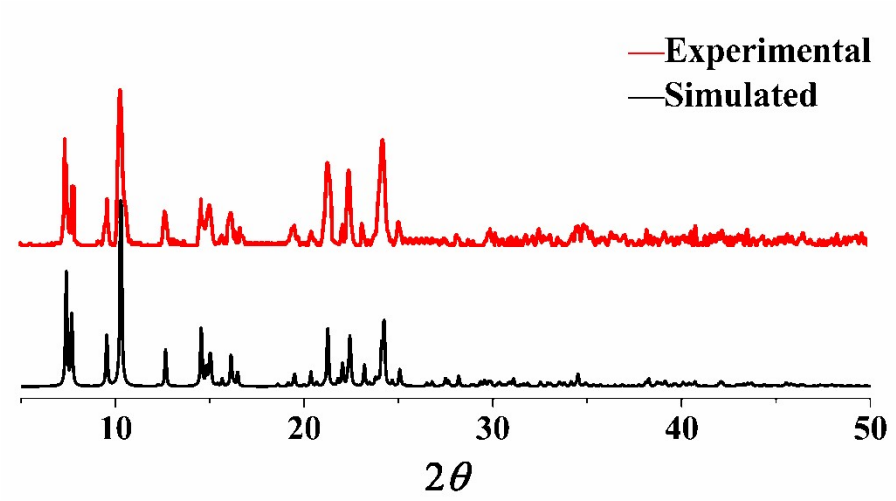

Fig. S4 PXRD patterns for complex **2**.

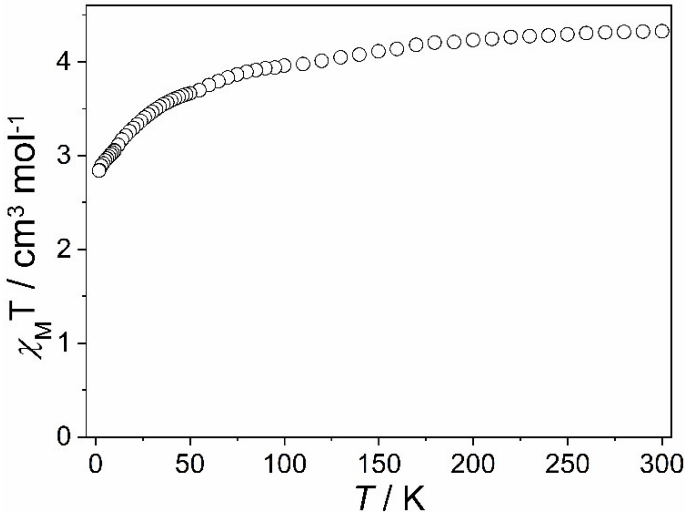

Fig. S5 Plots of $\chi_m T$ versus T for complex **1**.

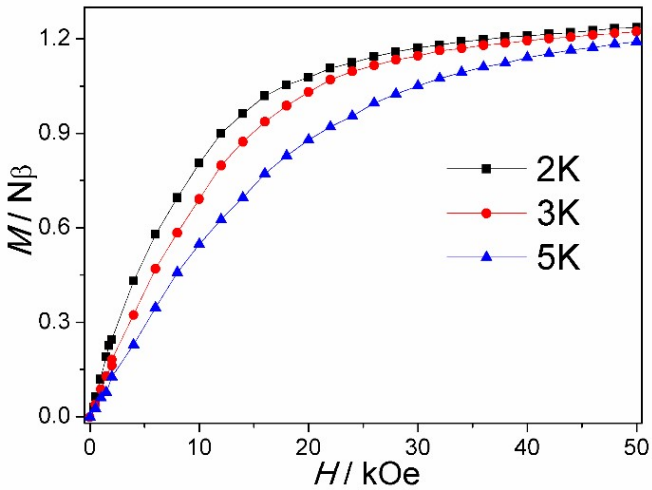

Fig. S6 Plots of M vs H curves for **2** at different temperatures. The solid lines represent fits to the data.

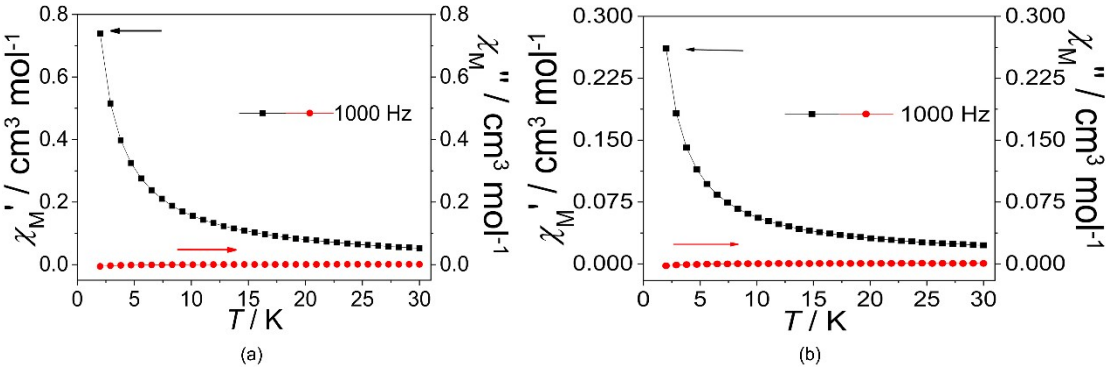

Fig. S7 Temperature dependence of χ'_M and χ''_M susceptibilities for **1** and **2** without static field.

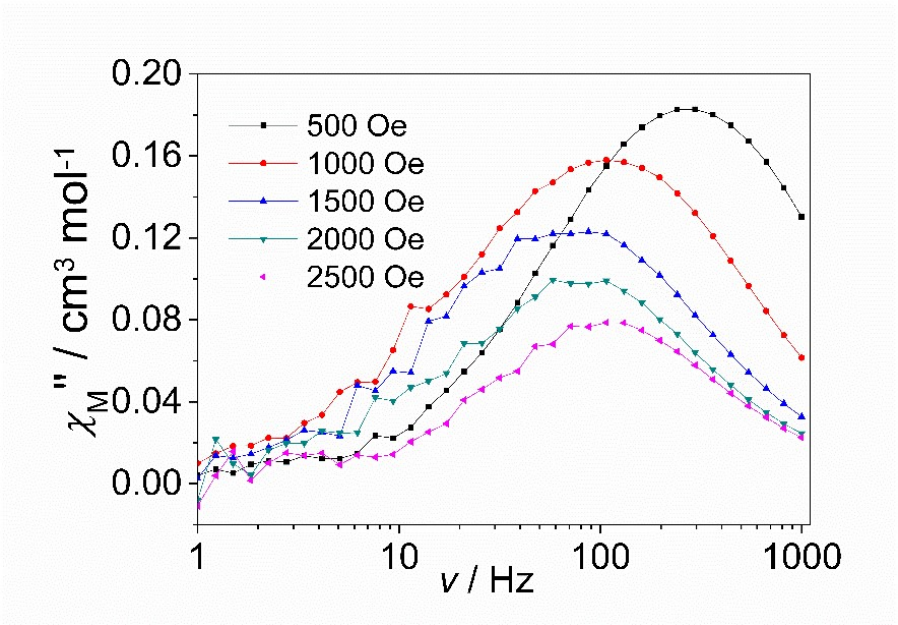

Fig. S8 The χ''_M for **2** at 2 K under different static fields.

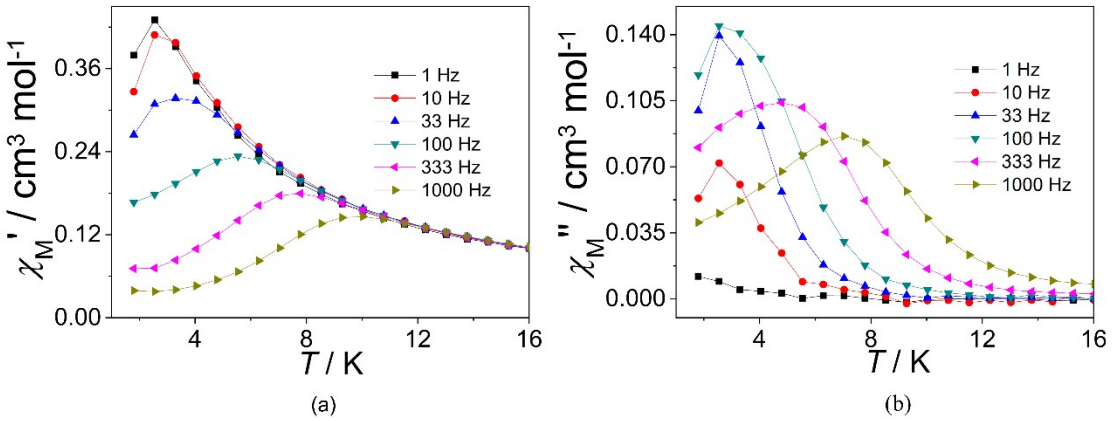

Fig. S9 Temperature dependence of χ'_M and χ''_M susceptibilities for complex **2** under a 1500 Oe dc field.

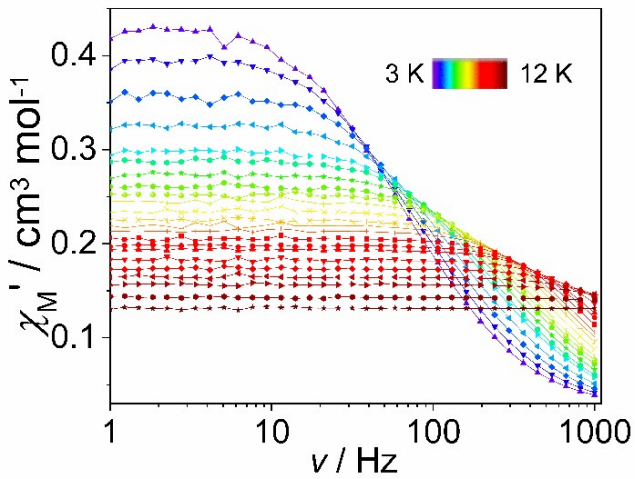

Fig. S10 Frequency dependence of the χ'_M susceptibility signals for complex **2** under a 1500 Oe dc field.

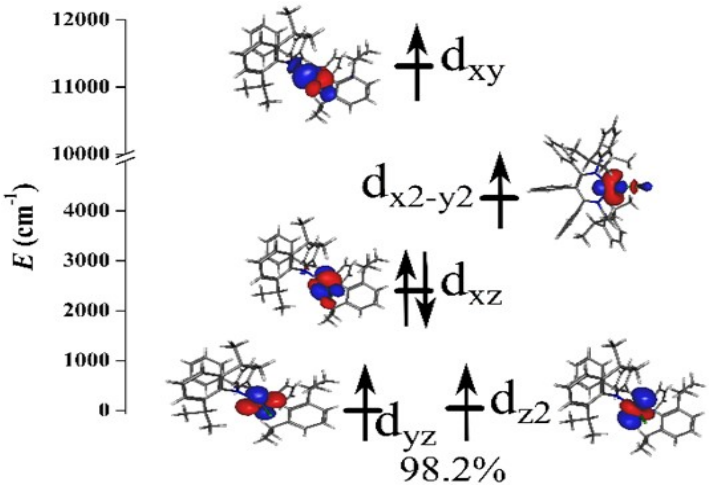

Fig. S11 Orbital energies computed for the ground state of **2** using CASSCF/RASSI-SO with ORCA 4.2. The percentage mention reveals the percent of the corresponding configuration mixing.

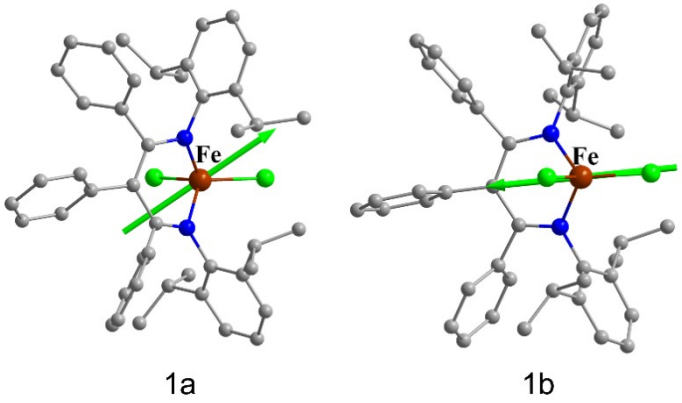

Fig. S12 Calculated orientations of the local main magnetic axes (green: g_z) on Fe^{III} ions of complexes **1** in their ground spin-orbit states.